ÓBUDAI EGYETEM
ÓBUDA UNIVERSITY

**Óbuda University**
**Doctoral School on Materials Sciences and Technologies**

# Modeling the Effect of Ultrasound on the Inelastic Deformation of Metals

**Dissertation Booklet**

for the degree of Doctor of Philosophy in Materials Science and Engineering at theDoctoral School of Materials Science and Technologies

**by**

**Ali H. Alhilfi**
M.Sc. in Materials Sciences and Engineering

**Supervisor**
**Prof. Dr. habil. Endre Ruszinkó**
University professor, Óbuda University

Budapest 2023

# I. Introduction

Since the early 20th century – Austrian scientists Blaha and Langenecker conducted the first tensile tests with superimposed ultrasound on a Zinc single crystal – the ultrasound-assisted processes have received rapidly increasing interest from academics and industries. Ultrasonic technology is a convenient and accessible assisting tool for many metalworking processes, such as machining, forming, joining, welding, microelectronic wire bonding, etc. Ultrasound shows various benefits: low energy consumption, high reliability and ampacity, short process time, etc. In addition, ultrasound finds ever-growing applications in the phase transformation processes of shape memory alloys.

# II. Objectives and State of Art

The objective set before the author is to develop a mathematical model for the analytical description of the inelastic deformation of metals in the ultrasound field. The following phenomena are considered:

## A. The effect of ultrasound on plastic deformation

*Acoustic Temporary Softening* is recorded during the simultaneous action of the unidirectional and oscillating load (acoustoplasticity). As a result, the decrease in the stress needed to develop plastic deformation is registered. (Blaha (1955), Kumar et al. (2017), Zohrevand et al. (2022)).

*Acoustic Residual Effects – residual hardening or softening* – are observed in the post-sonicated state of the material. Two possible outcomes are observed depending on the evolution of the material's defect structure during the acoustoplasticity. Materials with high stacking fault energy (SFE) demonstrate residual hardening – greater stress is needed to continue plastic straining after the acoustoplasticity (Deshpande et al. (2018, 2019)). Materials with low SFE show a reverse pattern – they flow at less stress in the post-sonicated period compared to the ordinary case. (Zhou et al. (2017), Kang et al. (2020)).

## B. The effect of ultrasound on time-depended processes

*Ultrasound-assisted creep* shows an essential increase in the deformation due to the inflow of acoustic energy. (Graff (2015), and Kulemin (1978)).

*Ultrasound-assisted relaxation of the cold-worked materials* manifests itself in a faster decrease in the yield strength/hardness of plastically deformed materials. (Kulemin (1978).

## C. The effect of ultrasound on the phase transformation in shape memory alloys

*Ultrasound-assisted austenite transformation* (*transformation plasticity*) demonstrates increases in deformation due to ultrasound impulses (Rubanik et al. (2008), and Bao et al. (2013)).

*Martensite transformation (pseudo elasticity) coupled with ultrasound energy* shows an increase in the stress needed to induce the transformation and modifies the kinetics of the stress-strain curve. (Rubanik et al. (2008), and Steckmann et al. (1999)).

Despite numerous experimental and numerical analyses about the potential benefits of applying ultrasonic energy, the underlying physical principles remain elusive. Two categories of the interpretation of the ultrasound effects can be indicated: (i) ***stress superposition*** and (ii) ***direct acoustic softening***.

Regarding the stress superposition theories, the softening effect results from the macroscopic superposition of steady and alternating stress. For example, Malygin (2000) implies that ultrasonic waves activate anchored dislocations hardened under ordinary deformation, reducing the stresses needed for further inelastic deformation.

At the same time, the superposition hypothesis can only partially explain the softening effect that occurs during ultrasonic vibration. The first reason for such a conclusion is the experimental results obtained by Daud et al. (2007), where the total amount of stress reduction on the stress-strain curve is generally higher than that of stress superposition alone. Furthermore, the superposition hypothesis cannot substantiate residual hardening or softening effects observed after ultrasonic vibration is stopped. These can be attributed to the permanent changes in the material's microstructure during ultrasonic sonication (direct acoustic softening). Deshpande et al. (2019), Lum et al. (2009), and Huang et al. (2009) suggest that these permanent changes are caused by dynamic annealing/softening induced by *heat input* from ultrasonic vibration. In other words, they draw an analogy between the effects of hot deformation and ultrasound action and indicate that similar microstructures evolve in thermal and ultrasonic fields.

Despite the debates between the supporters of stress superposition and direct acoustic softening, the researchers agree that ultrasound effects are contributed by both factors (Graff, 2015).

With ultrasound-assisted phase transformations, similar reasons are provided. Acoustic energy increases the mobility of interfaces (phase and domains) by decreasing the efficient friction force caused by alternate stresses. The superposition of alternate stresses induces the movement of interface and martensitic domain boundaries. In addition, ultrasonic heating of the sample can explain the variation in austenite deformation due to ultrasound waves' energy dissipation. (Klubovich et al. 1997, Rubanik et al. 2008, and Steckmann et al. 1999).

The phenomena considered above have been modeled in terms of the Synthetic theory of inelastic deformation, whose short review is presented below.

## III. The Synthetic Theory of Inelastic Deformation

The Synthetic theory incorporates the Budiansky slip concept (Batdorf & Budiansky, 1949) and Sanders's flow theory (Sanders, 1954) and works in the three-dimensional stress deviator space ($\mathcal{S}^3$), Rusinko, A. & Rusinko, K. (2009, 2011). Inelastic deformation at a point of the body is determined via deformations at the micro level of material, i.e., as a sum of inelastic deformations developed in active microvolumes (slip systems for plastics/creep deformation or domains involved in phase transformation):

$$\vec{\boldsymbol{e}} = \iiint_V \varphi_N \vec{\boldsymbol{N}} dV, \tag{3.1}$$

where $\varphi_N$ – inelastic strain intensity – an average measure of inelastic deformation occurring within one microvolume, and $\vec{\boldsymbol{N}}$ gives the orientation of this microvolume. One of the synthetic theory's main features is that the strain intensity relates to the carriers of inelastic deformation (dislocations, twins, point defects, etc.). This fact is mirrored in the following differential equation:

$$d\psi_N = r d\varphi_N - K\psi_N dt, \tag{3.2}$$

where $\psi_N$ – defect intensity – an average measure of defects developed within one microvolume; $r$ is the model constant, $t$ is time, and $K$ is a function of acting stress and temperature. The defect intensity is defined as

$$\psi_N = \left(\vec{\boldsymbol{S}} \cdot \vec{\boldsymbol{N}}\right)^2 - I_N^2 - S_P^2, \tag{3.3}$$

where $\vec{\boldsymbol{S}}$ is the stress vector, $S_P$ is a creep strength of the material, and $I_N$ is a rate integral:

$$I_N(t) = B \int_0^t \frac{d\vec{\boldsymbol{S}}}{ds} \cdot \vec{\boldsymbol{N}} \exp\big(-p(t-s)\big) ds, \tag{3.4}$$

where $B$ and $p$ are model constants.
While Eqs. (3.2)-(3.4) are applied for the modeling of plastic/creep deformation, for the case of phase transformations, the strain intensity is defined via the rate of martensite fraction (Φ) as

$$r\dot{\varphi}_N = \dot{\Phi}. \tag{3.5}$$

For martensite transformation, $\dot{\Phi}$ is

$$\dot{\Phi} = -\frac{\dot{T}_e}{M_s - M_f}, \qquad \dot{T}_e < 0 \text{ and } M_f < T_e < M_s. \tag{3.6}$$

For austenite transformation, $\dot{\Phi}$ is

$$\dot{\Phi} = -\frac{\dot{T}_e}{A_f - A_s}, \qquad \dot{T}_e > 0 \text{ and } A_s < T_e < A_f, \tag{3.7}$$

In the formulae above, $M_s$ and $M_f$ are the martensite transformation start and finish temperatures, respectively; $A_s$ and $A_f$ are the austenite transformation start and finish temperatures, respectively; $T_e$ is effective temperature defined as

$$T_e = T\left(1 - D\vec{\boldsymbol{S}} \cdot \vec{\boldsymbol{N}}\right), \tag{3.8}$$

where $D$ is a model constant.

## IV. Novel scientific results

# THESIS I

**In terms of the Synthetic theory, a model for the analytical description of the plastic flow of metals in the ultrasound field has been developed. The extension of the Synthetic theory is conducted by inserting into its governing relationships a term accounting for the effect of ultrasonic energy on the mechanical properties of materials. The proposed extension leads to correct results when considering the following phenomena [1-4]:**

- **(i) Stress drop on the stress~strain diagram as the ultrasound is On**
- **(ii) Acoustoplasticity – stress~strain diagrams under the simultaneous action of unidirectional and vibrating load**
- **(iii) Ultrasound residual hardening/softening – stress~strain diagram for the post-sonicated state of the metals**

In order to model the effects of ultrasound on the plastic deformation of metals listed above, Eq. (3.3) – the equation that governs the development of the carriers of inelastic deformation, the defects of the crystalline grid – is extended by two terms, $U_t$ and $U_r$:

$$\psi_{NU} = H_N^2 + U_t^2 + f(\gamma)U_r^2 - S_S^2, \tag{4.1.1}$$

where $U_t$ stands for the ultrasound-induced effects under the simultaneous action of static and ultrasound load (temporary effects), and $U_r$ is responsible for the deformation state of the material after the sonification (residual effect). The function $f(\gamma)$ standing as a factor before the term $U_r$ reflects the defect pattern of the material as a function of its stacking fault energy ($\gamma$).

The logic for the presentation of $U_t$ is dictated by the kinematics of the nucleation and multiplication of the crystal's imperfections in the ultrasound field. According to numerous experiments, e.g., Rusinko (2012), Kulemin (1978), etc., ultrasonic defect intensity increases as a function of the ultrasonic energy intensity and time. A power function can model the impact of the former factor, and the latter can be mathematically described through an exponential function, which mirrors that the ultrasonic defect intensity comes to saturation with sonication time. Therefore, the term $U_t$, responsible for the inelastic deformation superimposed by acoustic vibrations, is presented as a product of ultrasound energy (power function) and sonication duration (exponential function):

$$U_t = A_1 U^{A_2}(2 - e^{-wt})\left(\vec{\boldsymbol{u}} \cdot \vec{\boldsymbol{N}}\right), \quad t \in [0, \tau] \tag{4.1.2}$$

where $\tau$ is the sonication duration, $U$ is ultrasound energy intensity, $\vec{\boldsymbol{u}}$ is a unit vector determining the type of ultrasonic impact (longitudinal, torsional, etc.), $A_1$, $A_2$, and $w$ are model constants to be chosen for the best fit between the model and experiment results.

The term $U_r$ is defined as

$$U_r = h(\varepsilon - U) \times A_3 \int_0^{\tau} U^{A_4} dt, \tag{4.1.3}$$

where $h$ is the Heaviside step function, $\varepsilon$ is any positive infinitesimally small number so that ultrasound of any intensity results in a negative value of $\varepsilon - U$ difference. The presence of $h(\varepsilon - U)$ function means that the term $U_r$ takes effect only after the ultrasound is off; $A_3$, $A_4$ are model constants.

Formula (3.2), which reduces to $\psi_N = r\varphi_N$ in the case of plastic deformation, together with (4.1.1) and (4.1.2), gives the strain intensity in the presence of ultrasound ($\varphi_{NU}$) as

$$\varphi_{NU} = \left(\vec{\boldsymbol{S}} \cdot \vec{\boldsymbol{N}}\right)^2 + A_1 U^{A_2}(2 - e^{-wt})\left(\vec{\boldsymbol{u}} \cdot \vec{\boldsymbol{N}}\right) - S_S^2, \tag{4.1.4}$$

where $S_S$ is the yield strength of a material. It is easy to see that introducing the positive term $A_1 U^{A_2}(2 - e^{-wt})\left(\vec{\boldsymbol{u}} \cdot \vec{\boldsymbol{N}}\right)$ makes it possible to hold the $\varphi_{NU}$ at a given value at less static stress $\vec{\boldsymbol{S}}$ compared to the case of ordinary load. This fact correctly expresses the experimental results recording that plastic deformation develops at less static load in the presence of ultrasound.

After the ultrasound is Off, due to the formula (4.1.3), the plastic strain intensity takes grows in the following form

$$\Delta\varphi_N = \left(\vec{\boldsymbol{S}} \cdot \vec{\boldsymbol{N}}\right)^2 + f(\gamma)\frac{3}{2}[A_3 U^{A_4}\tau]^2 - S_S^2 - \varphi_{NU}. \tag{4.1.5}$$

If $f(\gamma) > 0$, we obtain the case of residual hardening when the plastic deforming in the post-sonicated state requires fewer stress values compared to the ordinary loading. The inequality $f(\gamma) < 0$ leads to the case of residual hardening when the material flows at greater values of the static stress after the ultrasound is Off. In the dissertation, the function $f(\gamma) > 0$ is defined via the linear function of the material stacking fault energy.

By using formulae (4.1.4) and (4.1.5), and (3.1), the plastic deformation and the corresponding stress~strain diagrams in the presence of ultrasound can be calculated and plotted, respectively.

The model results obtained within THESIS I correctly correlate with the following experimental recordings:

(i) The magnitude of the stress drop caused by the switching of the ultrasound increases with the ultrasound intensity: Fig. 4.1.

(ii) The material flow with superimposed ultrasound occurs at fewer stress values than the static load alone: Fig. 4.2, portions 2-3 and 6-7. The decrease in static stress increases with the ultrasound intensity/ amplitude: see Figs. 4.4 and 4.5.

(iii) The extended synthetic theory catches the phenomenon of residual hardening: see 3-4 portion in Fig. 4.2, where the plastic deformation in the post-sonicated state develops at greater stress values compared to the case of static loading. At the same time, too short sonification ($\tau = 2$ s for 6-7-8 portion) gives no residual hardening effect, which is explained by the ultrasound energy is not enough to nucleate such a stable defect structure to hamper the plastic flow in the post-sonicated state.

(iv) The model results for residual hardening are presented in Fig. 4.3, where the stress~strain diagram after the sonication runs beneath that obtained for the static load alone.

(v) Figs. 4.4 and 4.5 show the residual hardening for aluminum (high SFE) and residual softening for titanium (low SFE). With the increase in ultrasound amplitude, both phenomena appear more clearly.

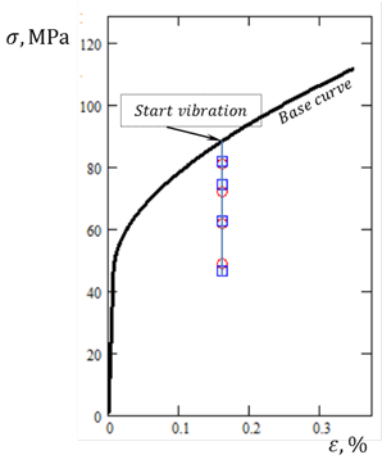


**Fig.4.1** Stress drops on the stress-strain diagram of aluminum caused by the switching of ultrasound with different intensities: $U_k = 5.89, 22.0, 60.33, 126.6\,\mathrm{J/m^3}$

(vi)

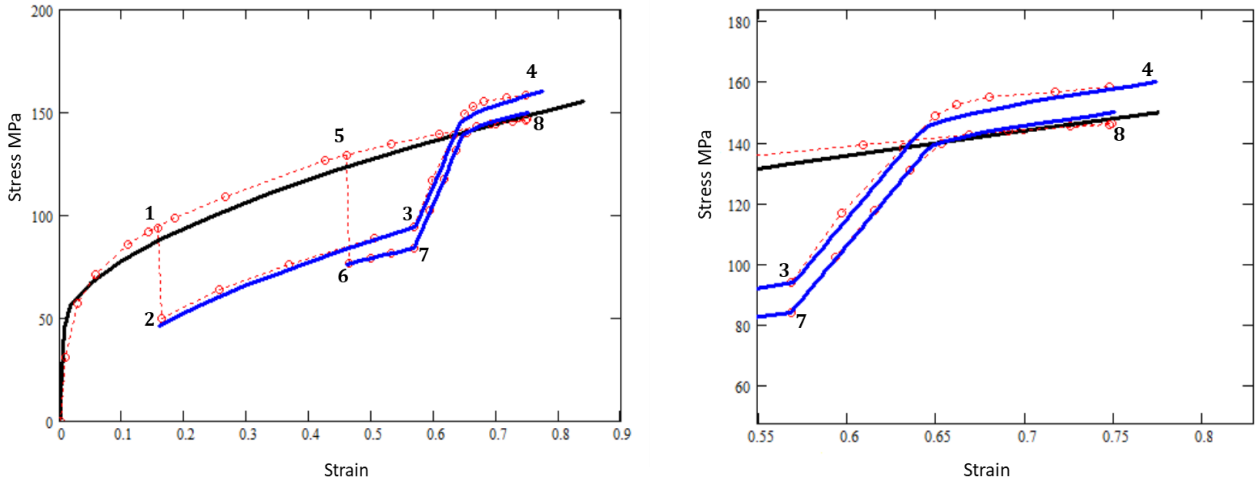


**Fig.4.2** Vibration-assisted stress~strain diagrams for aluminum in compression for ultrasound intensity $U = 126.6\,\mathrm{J/m^3}$; sonication time $\tau = 8$ s for 2-3-4 portion and $\tau = 2$ s for 6-7-8 portion; lines – model, ○ – experiment (Yao et al., 2012)

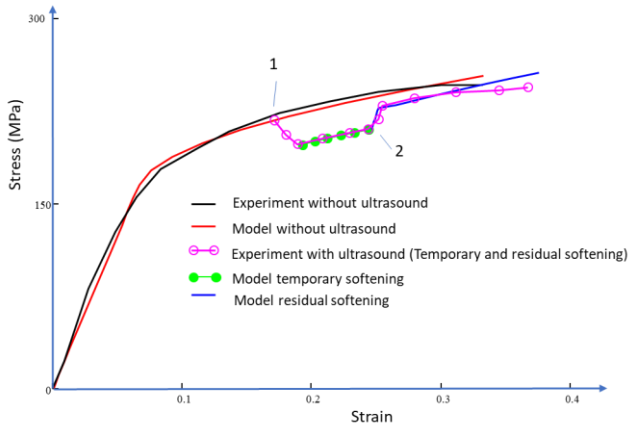


**Fig. 4.3** Vibration-assisted stress~strain compression diagrams for copper; ultrasound amplitude 1.3 μm.

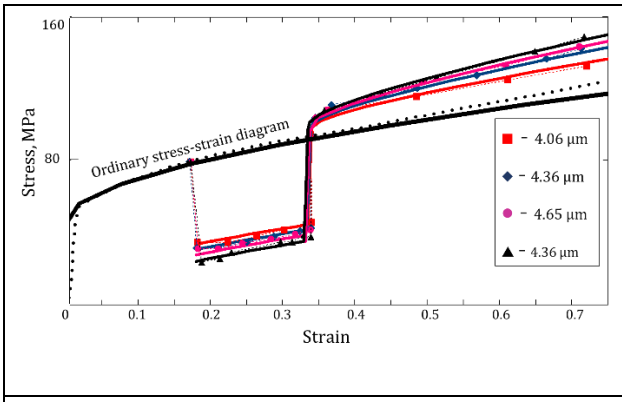


**Fig. 4.4.** Stress~strain compression diagrams of aluminum in the ultrasonic field (points – experimental data, Zhou et al. (2017); lines – model curves).

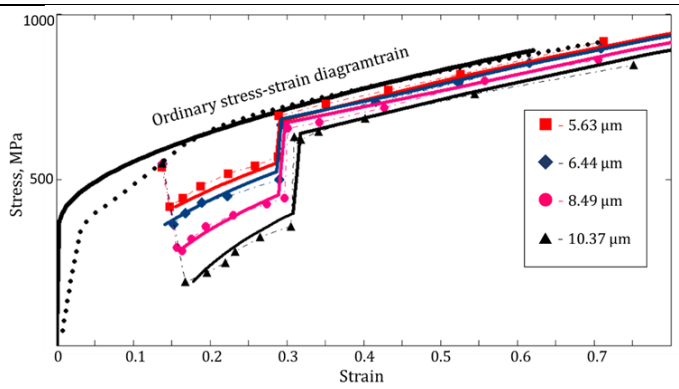


**Fig. 4.5** Stress~strain compression diagrams for titanium in the ultrasonic field (points – experimental data, Zhou et al. (2017); lines – model curves).

# THESIS II

**In terms of the Synthetic theory, a model for the analytical description of the ultrasound-assisted temporary deformation processes has been developed. The extension of the Synthetic theory is conducted by inserting into its governing relationships a term accounting for the effect of ultrasonic energy on the mechanical properties of materials. The obtained results show good conformity between the model and experimental data for the following phenomena [5-7]:**

- **(i) The increase in primary creep under the periodic and continuous action of ultrasound**
- **(ii) The increase in secondary creep in an acoustic field**
- **(iii) Ultrasound-induced relaxation (recovery) of the work-hardened materials**

Adhering to the overall concept of modeling ultrasound's effect on inelastic deformation, the basic relationship of the synthetic theory, Eq. (3.3), is to be extended by the term ($U_C$) responsible for acoustic energy:

$$\psi_N = H_N^2 - I_N^2 - S_P^2 + U_C^2, \tag{4.2.1}$$

$$U_C = \vec{\boldsymbol{u}} \cdot \vec{\boldsymbol{N}}, \tag{4.2.2}$$

$$\vec{\boldsymbol{u}} = C_1 {S_m}^{C_2} (1 - e^{-wt}) \vec{\boldsymbol{u}}, \tag{4.2.3}$$

where $S_m$ is the ultrasound stress amplitude. Again, one can see the two elements in the above formula – $C_1 {S_m}^{C_2}$ and $e^{-wt}$ – that reflect the behavior of the defects of crystalline grid nucleated by ultrasound. The former reflects the dependence of ultrasound defects on the ultrasound intensity (ultrasound stress amplitude), and the latter their temporary development.

The above formulae, together with Eqs. (3.1) and (3.2), are proposed to be used to describe ultrasound-assisted primary creep. The logic of the appearance of the term $U_C$ is clear. Since, during primary creep, Eq. (3.2) gives $\varphi_N = \psi_N / r$, the introduction of the term $U_C$ will model the increase in creep deformation caused by the ultrasound.

To catch the phenomena recorded at the superposition of ultrasound on the A) secondary creep and B) the relaxation processes, the

following is proposed.

A) The creep rate within one slip system is obtained from (3.2) as $r\dot{\varphi}_N = K\psi_N$.

B) The relaxation of work-hardened material, i.e., the decrease in the defects cumulated in plastic flow, is derived from (3.2) as $d\psi_N = -K\psi_N dt$.

In order to reflect an accelerating effect of the acoustic energy on the above processes, the function $K$ from (3.2) is extended by the term containing the ultrasound stress amplitude $S_m$:

$$K_U = K + R_1(S_m H_{\max})^{R_2}, \tag{4.2.4}$$

where $H_{\max}$ reflects the magnitude of plastic deformation prior to the relaxation; (for the creep $H_{\max} = const =$ acting stress). The product $S_m H_{\max}$ in (4.2.4) symbolizes that the promoting action of ultrasound increases with the deformation energy cumulated in the material.

The model results obtained within THESIS II – derived from (3.1) and (4.2.1)-(4.2.4) – show good agreement with the following experimental data:

(i) Ultrasound energy increases the primary creep deformation: see Figs. 4.6 and 4.7. Fig. 4.6 demonstrates that this phenomenon escalates with the ultrasound stress amplitude.

(ii) In the case of periodic sonication (Fig. 4.7), the values of deformation increments decay with the number of ultrasound switches, and there comes the point when the ultrasound exerts no effect. In this phenomenon, the temporary behavior of ultrasound defects (their number first increases and then goes to saturation) is most evident.

(iii) Ultrasound superimposition causes an increase in primary and secondary creep deformation, which is seen in the increase of the slope angle of creep diagrams in Fig. 4.8.

(iv) Ultrasound energy induces the relaxation processes for the materials subjected to plastic deformation, which becomes more evident as plastic deformation grows. So, Line 2 in Fig. 4.9 shows a steeper hardness decrease than Line 1 (without the ultrasound, the recovery of the work-hardened material at room temperature is not observed).

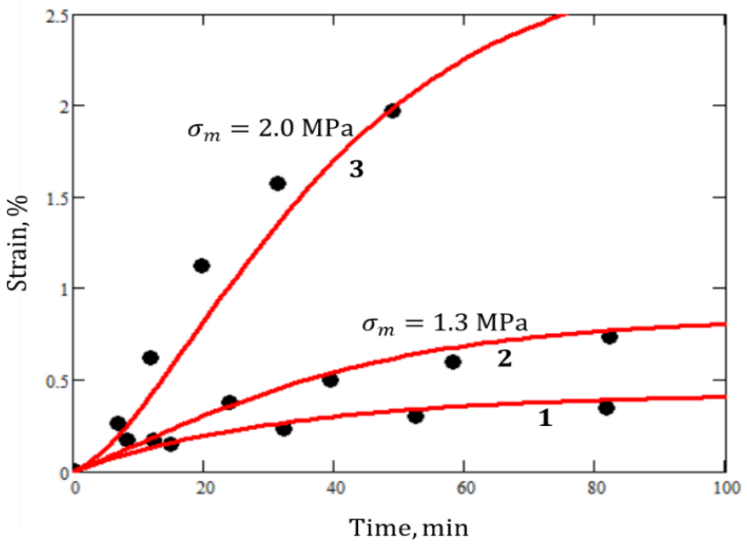


**Fig. 4.6** Strain vs. Time diagrams of aluminum in uniaxial tension ($\sigma = 10$ MPa, $T = 40$°C): 1 – ordinary creep, 2 and 3 – ultrasound-assisted creep with continuous sonication, • – experiment (Kulemin, 1978), lines – model.

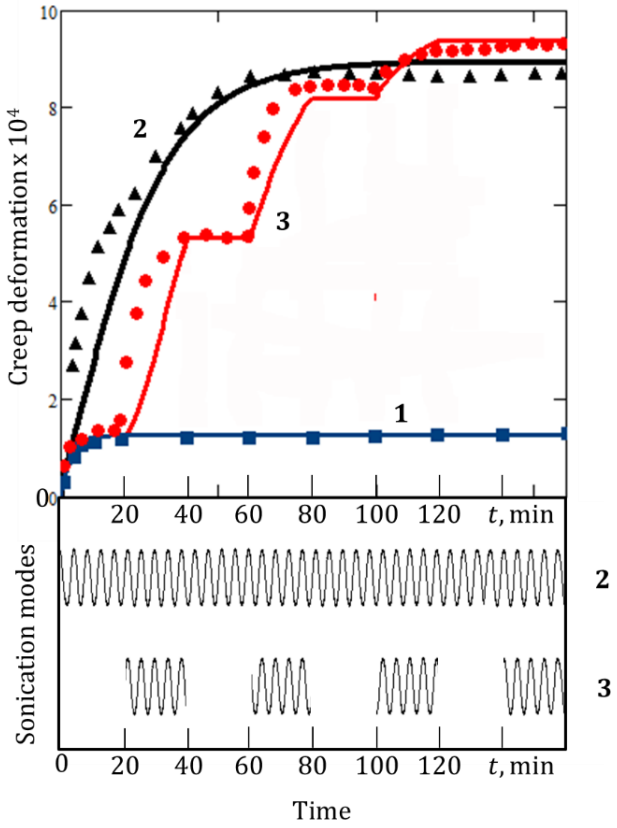


**Fig. 4.7** Strain vs. Time diagrams of copper: **1** – ordinary creep, **2** – ultrasound-assisted creep ($\sigma_m = 2.6$ MPa) with continuous sonication, **3** – ultrasound-assisted creep with periodic sonication; symbols – experiment (Kulemin, 1978), lines – model.

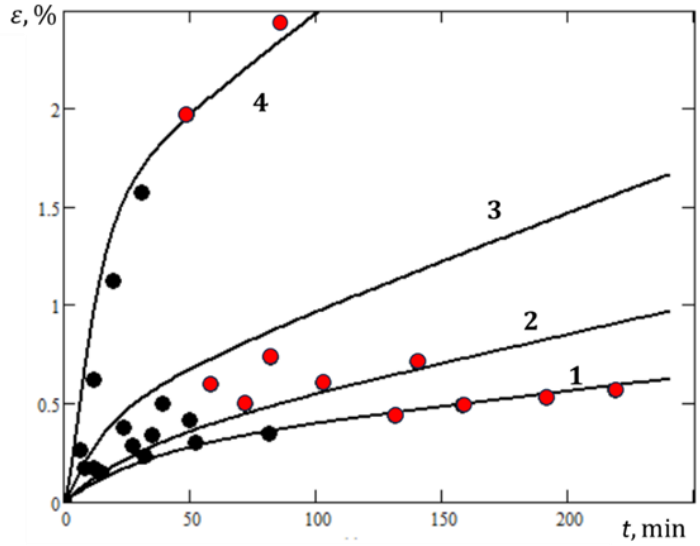


**Fig. 4.8** Creep diagrams of aluminum in uniaxial tension ($\sigma = 10$ MPa, $T = 40$°C), 1 – ordinary creep, 2-4 ultrasound-assisted creep with oscillating stress amplitudes of 0.6 MPa (2), 1.3 MPa (3), and 2.0 MPa (4); ● – experiment (Kulemin, 1978), lines – model.

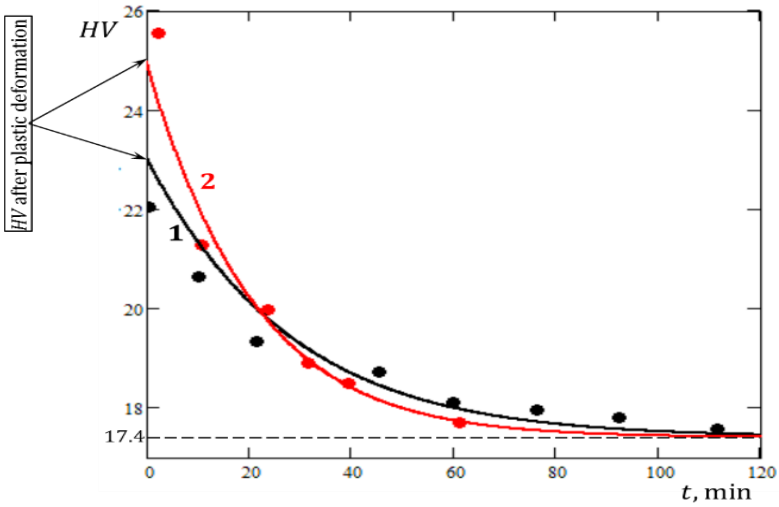


**Fig. 4.9** *HV* vs. *sonication time* plots for the plastically deformed aluminum specimen: $\varepsilon_1 = 3.6$ % and $\varepsilon_2 = 6.8$ %, $t = 20$℃; • – experiment (Kulemim, 1978), lines – model

## THESIS III

**In terms of the Synthetic theory, a model for the analytical description of the ultrasound-assisted phase transformations of the shape memory alloys has been developed. The extension of the Synthetic theory is conducted by inserting into its governing relationships a term accounting for the effect of ultrasonic energy on the mechanical properties of materials. The model results correctly correlate with experimental recordings for the following phenomena [8-10]:**

**(i) Ultrasound impulses induce strain drops during austenite transformation (transformation plasticity)**

**(ii) Ultrasound superimposed on a static load decreases stresses needed to start martensite transformation during pseudoelastic deformation**

In terms of the Synthetic theory, the phenomena of transformation plasticity and pseudoelasticity are modeled via Eqs. (3.1) and (3.5)-(3.8), where the effective temperature, being a function of acting stress and temperature, plays a central part. It is, therefore, appropriate to extend the relationship for $T_e$ by a term reflecting the presence of ultrasound:

$$T_e = T\left(1 - D\vec{\boldsymbol{S}} \cdot \vec{\boldsymbol{N}}\right) \pm U, \tag{4.3.1}$$

where the sign "+" is applied for austenite and "–" for martensite transformation. It is clear that the term $U$ promotes both transformations: while the increment in the effective temperature intensifies austenite transformation, the reduction in $T_e$ does martensite transformation.

The general line, which states that the impact of ultrasound is primarily proportional to the vibrating stress amplitude $\vec{\boldsymbol{S}}_m$ (ultrasound intensity), remains unchangeable. All other modifications relate to the peculiarities of direct (martensite) and reverse (austenite) transformation.

In the case of the ultrasound-assisted transformation plasticity, as $\sigma = const$ and $\dot{T} > 0$, the following formulae are proposed

$$U = \left(B + e^{-w(T-T_i)}\right) \int_{A_s}^{T} (f \cdot g) dt, \tag{4.3.2}$$

$$f = U_1\left(\vec{S}_m \cdot \vec{N}\right), \tag{4.3.3}$$

$$g = \frac{a^3}{a^2 + (T-C)^2}, \tag{4.3.4}$$

where $a$, $B$, $C$, and $U_1$ are model constants. Function $g$ from (4.3.4) reflects the experimental fact that the effect from the ultrasound varies with the temperature when it is applied. The term $\left(B + e^{-w(T-T_i)}\right)$ is devoted to modeling the peculiarities of the deformation after the ultrasound is switched Off.

In the case of ultrasound-assisted pseudoelasticity, as $\dot{\sigma} > 0$ and $T = const$, the following formulae are proposed

$$U = U_1\left(\vec{S}_m \cdot \vec{N}\right), \tag{4.3.5}$$

$$r_U = r + U_2|S_m|. \tag{4.3.6}$$

The introduction of $r_U$ is driven by the necessity to catch the experimentally registered fact that the slope of $\sigma{\sim}\varepsilon$ curve reacts on the martensite transformation stage, i.e., ultrasound's influence varies during the transformation (Malygin 2001, Sapozhnikov et al. 1996, Steckmann et al. 1999)

The plots presented within THESIS III – constructed via Eqs. (3.1), (3.5)-(3.8) and (4.3.1)-(4.3.6) – demonstrate a good fit of the model to the following experimental data:

(i) Ultrasonic vibrations impulsively added to austenitic transformation result in negative strain jumps. In other words, acoustic energy can initiate strain variations of SMA (Fig. 4.10). The magnitude of the strain jumps increases with the ultrasonic vibration amplitude.

(ii) The effect of insonation strongly depends on the moment the ultrasound is applied. Acoustic energy has no effect if it acts outside the austenite transformation temperature range. Further, the magnitude of the ultrasound-induced strain jumps is not distributed uniformly within the austenite transformation temperature range. This phenomenon reaches its maximum if the alternate stresses are applied approximately in the middle of the temperature range of phase transformations (Figs. 4.10 and 4.11).

(iii) The finish temperature is less than during conventional heating. In other words, the temperature needed to finish the transformation is partially compensated by ultrasound heating. (Fig. 4.10)

(iv) After switching of ultrasound, the further realization of SME occurs according to the reverse transformation kinetics. However, immediately after the ultrasound is off, some "backsliding" in austenitic deformation, a slight increase of deformation, is observed (Fig. 4.10). This aftereffect is assumed to be due to a) the decrease in temperature after ultrasound is off and b) the action of ultrasound which "left a trail" in the form of ultrasound-assisted defect conglomeration, reducing the development of the phase transformations. Therefore, while the central portion of acoustic energy converts irreversibly into the phase deformation increment, some fraction of it recovers.

(v) In the presence of ultrasound, the start stress needed to induce and produce martensite transformation in a pseudoelastic experiment is less than that in the ordinary load (Fig. 4.12).

(vi) At the end of the martensite transformation, the $\sigma{\sim}\varepsilon$ curve shows steeper kinetics than without ultrasound (Fig. 4.12)

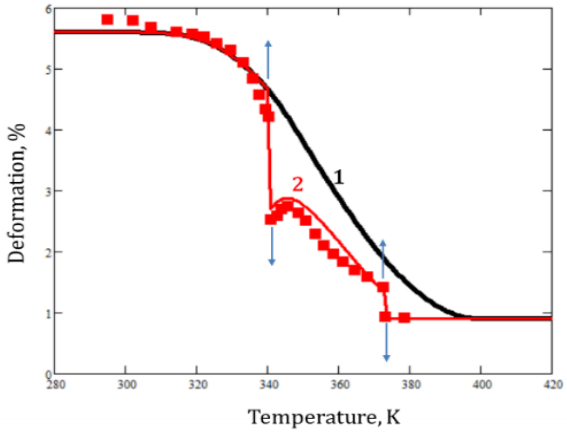


**Fig. 4.10** State diagram of NiTi alloy in Deformation-Temperature coordinate. The sample is subjected to uniaxial tension $\sigma =$ 30 MPa. The arrows show the moments of switching-on (↑) and switching-off (↓)of ultrasonic vibrations with amplitude 8.3 MPa; ■ –experiment (Rubanik et al., 2008), lines – model.

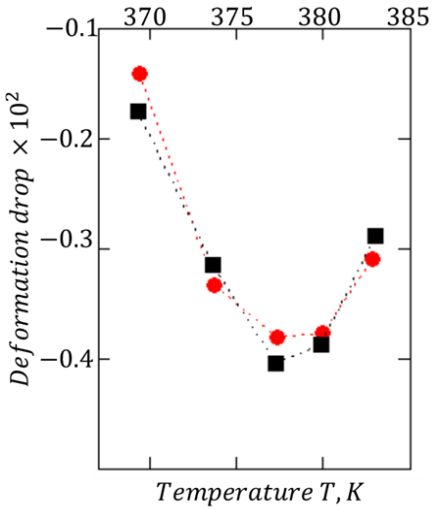


**Fig. 4.11** Ultrasound-induced deformation drops in the course of austenitic reverse thermoelastic phase transformation; the amplitude of ultrasonic deformation at every impulse $\varepsilon_m = 5 \times 10^{-5}$ ● – experiment (Steckmann et al. 1999), ■ – model results

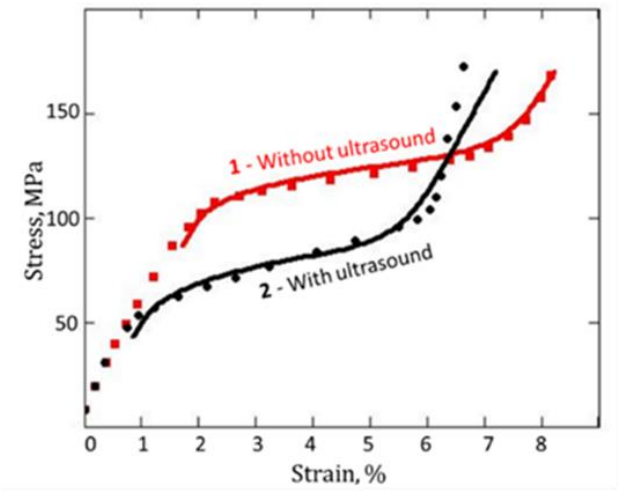


**Fig. 4.12** Pseudoelastic σ~ε diagram of NiTiRe alloy at constant temperature ($T_0 = 283$ K) in uniaxial tension: 1 – static loading, 2 – simultaneous action of static and ultrasonic loading ($\sigma_m = 16$ MPa). Lines – model, symbols – experiment (Steckmann et al., 1999).

## V. Conclusion

All the objectives set before the dissertation's author are fully implemented. A wide range of issues has been studied and modeled, namely ultrasound-assisted

a) plastic deformation,
b) primary and secondary creep; relaxation processes,
c) phase transformation.

The Synthetic theory, which is taken for a mathematical apparatus, has proved itself as a reliable analytical mechanism to model various non-classical problems in the field of solid mechanics.

## References


Bao, M., Zhou, Q., Dong, W., Lou, X., Zhang, Y. (2013) Ultrasound-modulated shape memory and payload release effects in a biodegradable cylindrical rod made of chitosan-functionalized PLGA microsphere, BioMac.

Batdorf, S. and Budiansky, B. (1949) A mathematical theory of plasticity based on the concept of slip, NACA, Technical note, 871.

Blaha, F., Langenecker, B., (1955), Dehnung von Zink-Kristallen unter Ultraschalleinwirkung. Naturwissenschaften 42,556.

Daud, Y., Lucas, M., & Huang, Z. (2007). Modelling the effects of superimposed ultrasonic vibrations on tension and compression tests of aluminium. Journal of Materials Processing Technology, 186(1-3), 179-190.

Deshpande, A., & Hsu, K. (2018). Acoustic energy enabled dynamic recovery in aluminium and its effects on stress evolution and post-deformation microstructure. Materials Science and Engineering: A, 711, 62-68.

Deshpande, A., Tofangchi, A., & Hsu, K. 2019. Micro-structure evolution of Al6061 and copper during ultra-sonic energy assisted compression. Materials Characterization, 153, 240-250.

Graff, K. F. (2015). Ultrasonic metal forming: Processing. In Power Ultrasonics (pp. 377-438). Woodhead Publishing.

Huang, H., Pequegnat, A., Chang, B. H., Mayer, M., Du, D., & Zhou, Y. 2009. Influence of superimposed ultrasound on deformability of Cu. Journal of Applied Physics, 106(11), 113514.

Kang, J., Liu, X., & Xu, M. (2020). Plastic deformation of pure copper in ultrasonic assisted micro-tensile test. Materials Science and Engineering: A, 785, 139364.

Kulemin, A. V. 1978. Ultrasound and Diffusion in Metals. Metallurgia Publ., Moscow.

Kumar, S., Wu, C. S., Padhy, G. K., & Ding, W. (2017). Application of ultrasonic vibrations in welding and metal processing: A status review. Journal of Manufacturing Processes, 26, 295–322.

Lum, I., Hang, C. J., Mayer, M., & Zhou, Y. (2009). In situ studies of the effect of ultrasound during deformation on residual hardness of a metal. Journal of electronic materials, 38(5), 647-654.

Malygin, G. 2000. Acoustoplastic effect and the stress superimposition mechanism. Physics of the Solid State,42(1), 72-78.

Rubanik Jr., V.V. Rubanik, V.V. Klubovich, V.V. (2008) The influence of ultrasound on the shape memory behavior, MSE A 481–482 620–622.

Rusinko, A., & Rusinko, K. (2011). *Plasticity and creep of metals*. Springer Science & Business Media.

Rusinko, A. (2012). *Ultrasound and Irrecoverable Deformation in Metals*: Modeling of Plastic and Creep Deformation. LAMBERT.

Sanders J. (1954) Plastic Stress-Strain Relations Based on Linear Loading Functions. Proceedings of the Second USA National Congress of Applied Mechanics, Ann Arbor, 14-18 June 1954, 455-460.

Steckmann, H., Kolomytsev, V.I., Kozlov, A.V. Acoustoplastic effect in the shape memory alloy Ni–Ti–Re at ultrasonic frequency, Ultrasonics 37 (1999) 59–62.

Yao, Z., Kim, G. Y., Faidley, L., Zou, Q., Mei, D., & Chen, Z. (2012). Effects of superimposed high-frequency vibration on deformation of aluminum in micro/meso-scale upsetting. Journal of Materials Processing Technology, 212(3), 640-646.

Zhou, H., Cui, H., Qin, Q. H., Wang, H., & Shen, Y. (2017). A comparative study of mechanical and microstructural characteristics of aluminium and titanium undergoing ultrasonic assisted compression testing. Materials Science and Engineering: A, 682, 376-388.

Zohrevand, M., Aghaie-Khafri, M., Forouzan, F., (2022). An investigation on microstructure and mechanical properties of 316 stainless steel: a comparison between ultrasonic treatment and thermal annealing. Philosophical Magazine, 1-23.

## List of Alhilfi's Publications


[1] Alhilfi, a., & Rusinko, a., (2022), Modelling of ultrasonic temporary and residual effects, *Journal of theoretical and applied mechanics, Sofia,* (52), 64-74. WoS, SCOPUS, Q3**, IF: 0.2**

[2] Alhilfi, A. H., & Rusinko, A. (2022). Ultrasonic temporary softening and residual hardening. *Engineering Review*: 42(2), 101-113. WoS, SCOPUS, Q4

[3] Ali H. Al Hilfi, Andrew Rusinko, (2022), Ultrasonic Temporary Softening And Residual Softening In Terms Of The Synthetic Theory, *AGTECO* 2021, Kecskemét, Hungary, Nov. 25-27, 202. Published in *Gradus* l9(2).

[4] Rusinko, A., & Alhilfi, A. H., (2020), Evolution of loading surface in the ultrasonic field, *Proceedings of the Engineering Symposium at Bánki*, pp. 35-40.

[5] Rusinko, A., & Alhilfi, A. H. (2021). Ultrasound-assisted creep deformation of metals. *Acta Periodica Technologica*, (52), 265-273. WoS, SCOPUS, Q3

[6] Rusinko, A., Alhilfi, A. H., & Rusinko, M. (2022). An analytic description of the creep deformation of metals in the ultrasonic field. *Mechanics of Time-Dependent Materials*, 26(3), 649-661. WoS, SCOPUS, Q2, **IF: 2.538**

[7] Ruszinko, E., & ALHILF, A. (2021). The Effect of Ultrasound on Strain-hardened Metals. *Acta Polytechnica Hungarica*, 18(8), 221-233. SCOPUS, Q2, **IF: 1.71**

[8] Alhilfi, A. H., & Rusinko, A. (2022). Austenite Transformation of Shape Memory Alloys in the Ultrasonic Field. *Mechanics of Solids*, 57(5), 1097-1103. WoS, SCOPUS, Q3, **IF: 0.5**

[9] Alhilfi, A. H., & Rusinko, A. (2022). Effect of Ultrasound on the Pseudoelasticity of Shape Memory Alloys. *Journal of Materials Science and Chemical Engineering*, 10(6), 1-12.

[10] Alhilfi, A. H., & Ruszinkó, E. (2023). Effect of Ultrasound on the Austenite Transformation of Shape Memory Alloys. *Acta Polytechnica Hungarica*, 20(4), 85-101. SCOPUS, Q2, **IF: 1.71**